NOTES AND CORRESPONDENCE

Autocorrelation Scales of the SST Distribution and Water Masses Stratification in the Channel of Sicily

GIANLUCA BORZELLI AND ROBERTO LIGI

Telespazio, Rome, Italy

17 April 1998 and 7 July 1998

ABSTRACT

A 1-yr-long series of Advanced Very High Resolution Radiometer sea surface temperature (SST) images is used to study the SST distribution in 1992 over the Channel of Sicily. Time- and spatial scales of the SST are studied by estimating the SST autocorrelation function directly from satellite images. SST timescales vary from 1 week to 45 days, with lower values in areas of intense upwelling. Spatial scales of the SST show seasonal variations with values from 80 to 300 km, with higher values during the summer. Oscillations with periods from 11 to 35 days modulate the annual variability of the SST spatial scales. The first four internal radii of deformation are estimated on the basis of climatological density profiles. The first internal radius varies from 7 km during the winter to 14 km during the summer. It is shown that, although differences between horizontal scales of the SST and internal radii of deformation exist, the annual variability of the SST spatial scales can be interpreted in terms of seasonal variations of the first Rossby radius of deformation.

1. Introduction

The Channel of Sicily (Fig. 1) is the channel through which water is exchanged between the Eastern and the Western Mediterranean. In the available literature, the vertical structure of the Channel of Sicily is described in terms of two layers: a surface layer of Atlantic Water (AW), flowing eastward, and a bottom layer of water of Levantine origin [Levantine Intermediate Water (LIW)], flowing westward. These waters mix in an intermediate region whose thickness varies seasonally from 100 m to a few dozen meters.

The Eastern Mediterranean is a ''negative'' basin within which evaporation exceeds precipitation and river runoff. In the long term, the AW inflow through the Channel of Sicily compensates the volume loss due to the LIW outflow and evaporation–precipitation deficit. Therefore, the Channel of Sicily plays an important role in controlling the circulation of the entire Mediterranean on the synoptic scale, and a detailed knowledge of the dynamic of this region is essential to the comprehension of the Mediterranean circulation.

An important summary of the oceanography of the Channel of Sicily has been given by Manzella et al. (1990). Comparing hydrographic and current meter data, these authors show evidence for an interesting relationship between the seasonal variability of SST and the currents over the Channel of Sicily. Following Manzella et al. (1990), the horizontal distributions of temperature and salinity in the channel are more uniform in the summer than in the winter. The enhanced horizontal uniformity is accompanied by a more uniform distribution of the mean velocity, mean kinetic energy, and eddy kinetic energy, with values increasing two to three times during the winter (see also Grancini and Michelato 1987). Thus, an analysis of the spatial and temporal scales of the SST over the Channel of Sicily, along with its seasonal variability, is essential in understanding the mechanisms regulating the water exchanges between the Eastern and Western Mediterranean.

A study of time and spatial scales of the SST distribution over the Channel of Sicily and its relationships with seasonal variations of water mass stratification is presented here. The study is based on an intensive analysis of a sequence of 187 daytime remotely sensed SST images, collected during 1992 (1 January–31 December) by the Advanced Very High Resolution Radiometer (AVHRR) on board the *National Oceanic and Aeronautics Administration NOAA–11* (*NOAA-11*) spacecraft. It is also based on climatological in situ data kindly supplied by Ente Nazionale Energia e Ambiente (ENEA)–Centro Ricerche Ambiente Marino in La Spezia, Italy.

Manzella et al. (1988), analyzing current meter data

Corresponding author address: Gianluca Borzelli, Telespazio, S.p.A., Via Tiburtina 965, 00156 Rome, Italy.
E-mail: gianluca@biolab.med.unisi.it

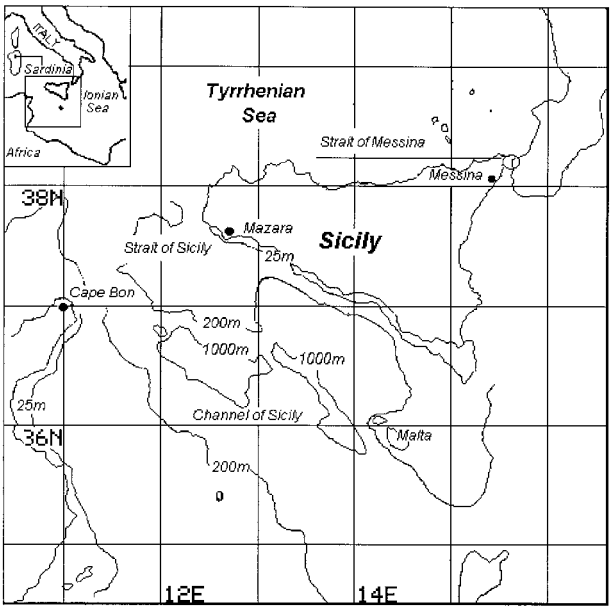

FIG. 1. Study area: the Channel of Sicily.

of the Strait of Sicily collected during the Western Mediterranean Circulation Experiment, show a high seasonal variability in the LIW transport in the channel. We have already seen that the structure of the SST field reflects the dynamic of the currents through the channel. It is not clear, however, how the variability of the presence of different water masses is related to characteristic scales of the SST autocorrelation function (ACF). When initiating synoptic studies in regions of the open ocean and when Brunt–Väisälä frequency profiles are available, it is common practice to represent characteristic scales of the SST ACF on the basis of an estimate of the internal deformation radius. However, this approach may fail in a region in which a strong seasonal signal is present. Indeed, although unstable modes tend to have scales on the order of the radius of deformation, energy tends to cascade on larger scales. In this situation, the dominant eddy scale tends to have an annual cycle similar to the Rossby radius annual cycle, but owing to the strong seasonal modulation, statistical equilibrium between different modes is not likely to be achieved, and these cycles may present significant differences. For example, over the Western Mediterranean, horizontal gradients are stronger in summer than in winter (Santoleri et al. 1994), associated with a shorter correlation length of the SST ACF. Conversely, in summer the increased vertical stratification produces a longer internal radius of deformation, causing contradiction in the modeling of the ACF in terms of internal deformation radius.

2. Data and methods

A total of 187 daytime images collected during 1992 (1 January–31 December) were analyzed. The data consist of 1.1-km-pixel resolution images, corrected for limb darkening (Cornillon and Stramma 1985) and the earth's curvature and then mapped to an equirectangular grid. Brightness temperatures supplied by AVHRR channels 4 and 5 were converted to SST with a standard split-window algorithm (McClain 1981). A 512×512 pixel section covering the Channel of Sicily was extracted from the entire AVHRR scene. Cloudy and anomalously warm pixels (Cornillon and Stramma 1985) were eliminated by applying the algorithm described by Leonardi et al. (1994). This algorithm is based on an edge detection and a comparison of satellite-retrieved SST with some reference temperatures. First, it is verified that SST values of individual pixels fall within given temperature intervals. Whenever a pixel shows a temperature less than or greater than the cutoff temperatures defined by the bounds of such intervals, it is flagged as cloudy or anomalously warm. Then the standard deviation about the mean spatial SST is calculated, disregarding the flagged pixels. The remaining pixels are analyzed by using the edge-detection algorithm, and discontinuities that produce temperature differences higher than three times the standard deviation are classified as cloudy or anomalously warm.

The edge detection has been discussed in detail by Cayula and Cornillon (1992), and here it suffices to say that it is based on the analysis of the statistical distribution of pixel intensities belonging to subwindows (generally overlapping) in which the original image is divided. Whenever a subwindow possesses a bimodal distribution of pixels intensities, a front is detected in that window. The problem with this algorithm is the availability of the temperature dataset for comparison with remotely sensed SST values. To construct a similar reference dataset, monthly means and standard deviations of climatological temperatures can be used. However, use of these data with their small variability in cloud detection cause it to reject too many good data.

An iterative approach was therefore used to adjust the reference temperature dataset. A first approximation temperature dataset consisting of 12 temperature intervals, with cutoff values from 3° to 30°C for every month, was chosen. This dataset was used as input for the algorithm to detect clouds and diurnal warming events. The result of this analysis was a first approximation series of SST images. By grouping all SST values from every image during the same month and then calculating month-by-month means and standard deviations, new intervals of temperatures were computed. The new intervals were used to initiate the next iteration. The iterative process was continued as long as the average temperatures and the standard deviations changed more than half a degree between one iteration and another. The converged dataset of temperatures is presented in Table 1. Owing to different distributions of diurnal warming and clouds during the different seasons, a different number of iterations were required to reach convergence in the different months. The number of iter-

TABLE 1. Range of variation of the SST during 1992.

Month	Cutoff temperatures °C (min–max)	Iterations
Jan	12°–18°	2
Feb	12°–17°	3
Mar	11°–16°	2
Apr	12°–18°	2
May	14°–20°	2
Jun	18°–24°	3
Jul	19°–27°	4
Aug	19°–29°	3
Sep	17°–27°	3
Oct	17°–26°	2
Nov	15°–24°	3
Dec	14°–21°	2

ations required to reach convergence are also presented in Table 1.

Finally, pixels of the original series of images were flagged as cloudy or anomalously warm by means of the algorithm described by Leonardi et al. (1994), using as cutoff temperatures the intervals of Table 1. Images with percentages of contaminated pixels higher than 70% were excluded, and remaining images formed a series of 136 SST maps irregularly sampled in space and time.

Characteristic temporal and spatial scales of the SST distribution were estimated as scales of the SST ACF. However, the estimation of the ACF of a field from data is difficult, since it implies the average over different samples of the field. Moreover, the symmetry property is hard to deal with using real data (Carter and Robinson 1987).

When large datasets of regularly sampled data are available and assumed to be homogeneous, stationary, and isotropic, these difficulties can be overcome by estimating the ACF as the inverse Fourier transform of the power spectra of the data.

The time series of SST images presented in this note constitutes an irregularly sampled dataset both in space and in time. Therefore, even with assumptions of stationarity, homogeneity, and isotropicity, the estimation of the ACF as the Fourier transform of the SST power spectra is difficult to make. To estimate the SST ACF at distance $r = |\mathbf{x}_i - \mathbf{x}_1|$ and lag $t = |t_j - t_m|$ it is necessary to evaluate the average $\langle T(\mathbf{x}_i, t_j)T(\mathbf{x}_1, t_m)\rangle$ over a suitable ensemble or over different samples of the product in brackets. Fixing the position and making the assumption of stationarity, every pair of SST values distant in time by t can be considered different samples for the time ACF at lag t. Similarly, fixing time and making the assumptions of homogeneity and isotropicity, every pair of SST values distant by r can be considered different samples for the spatial ACF at distance r. By averaging these sample products, 512 × 512 (less land pixels) lookup tables of the SST time correlation and 136 lookup tables of the spatial correlation were obtained. Scales of the SST distribution were obtained by fitting time and spatial scales of correlation with a Gaussian model function of the form

$$C(r, t) = e^{-[r/\rho(t)]^2 - [t/\tau(x,y)]^2}, \quad (1)$$

obtaining a set of 512 × 512 (less land pixels) correlation times and 136 correlation lengths.

To interpret the temporal variability of the correlation length, internal radii of deformation were computed. In a stratified fluid, vertical motion is produced by the accommodation of the fluid under the action of the gravity field (Gill 1982). The equation that governs the vertical motion of a fluid parcel is the Sturm–Liouville eigenvalue problem (e.g., Tricomi 1961):

$$\frac{d^2w}{dz^2} + \frac{N^2(z)}{c^2}w(z) = 0, \quad (2)$$

with normal boundary conditions

$$w(0) = w(-H) = 0. \quad (2a)$$

In (2), w is the vertical velocity, $N(z)$ is the Brunt–Väisälä frequency $[N^2(z) = -(g/\rho)d\rho/dz\ (\text{rad s}^{-1})^2]$, and $1/c_n^2$ is the nth eigenvalue, with c_n representing the phase velocity of the nth normal mode. The Brunt–Väisälä angular frequency vertical profiles were calculated from climatological monthly mean density profiles kindly supplied by G. Manzella from the ENEA–Centro Ricerche Ambiente Marino. (Picco 1988). Equation (2) was solved with an ordinary finite-difference method for eigenvalue problems (e.g., Dahlquist and Bjorck 1974). Internal Rossby radii were calculated as $R_n = c_n/f$, in which f is the Coriolis factor expressed in rad s^{-1} (for midlatitude $f = 10^{-4}$ rad s^{-1}).

3. Results

The image of correlation times (Fig. 2) is characterized by noisy values distributed around a mean value of approximately 37 days. The only relatively organized pattern extends offshore from the Sicilian coasts for roughly 90–100 km over the continental shelf, where values range from 7 to 8 days near the coast to 25–30 days offshore. In Fig. 3 the time variation of the correlation lengths is shown. Outliers were eliminated by disregarding every point outside the interval $\langle R\rangle \pm 1.5\delta R$, where $\langle R\rangle$ represents the annual mean of the correlation length and δR represents the standard deviation.

To identify harmonic oscillations of the SST correlation length, a harmonic regression of the data presented in Fig. 3 (dots) was performed. The dataset was fitted with a standard chi-squared method with a superposition of simple harmonics. The number of simple harmonics along with their frequencies were chosen by computing the FFT transform of the linearly interpolated dataset of correlation lengths and selecting the most important oscillatory constituents. The superposition of simple harmonics mimicking the dataset is shown in Fig. 3 (solid line). In Table 2 the periods along with the

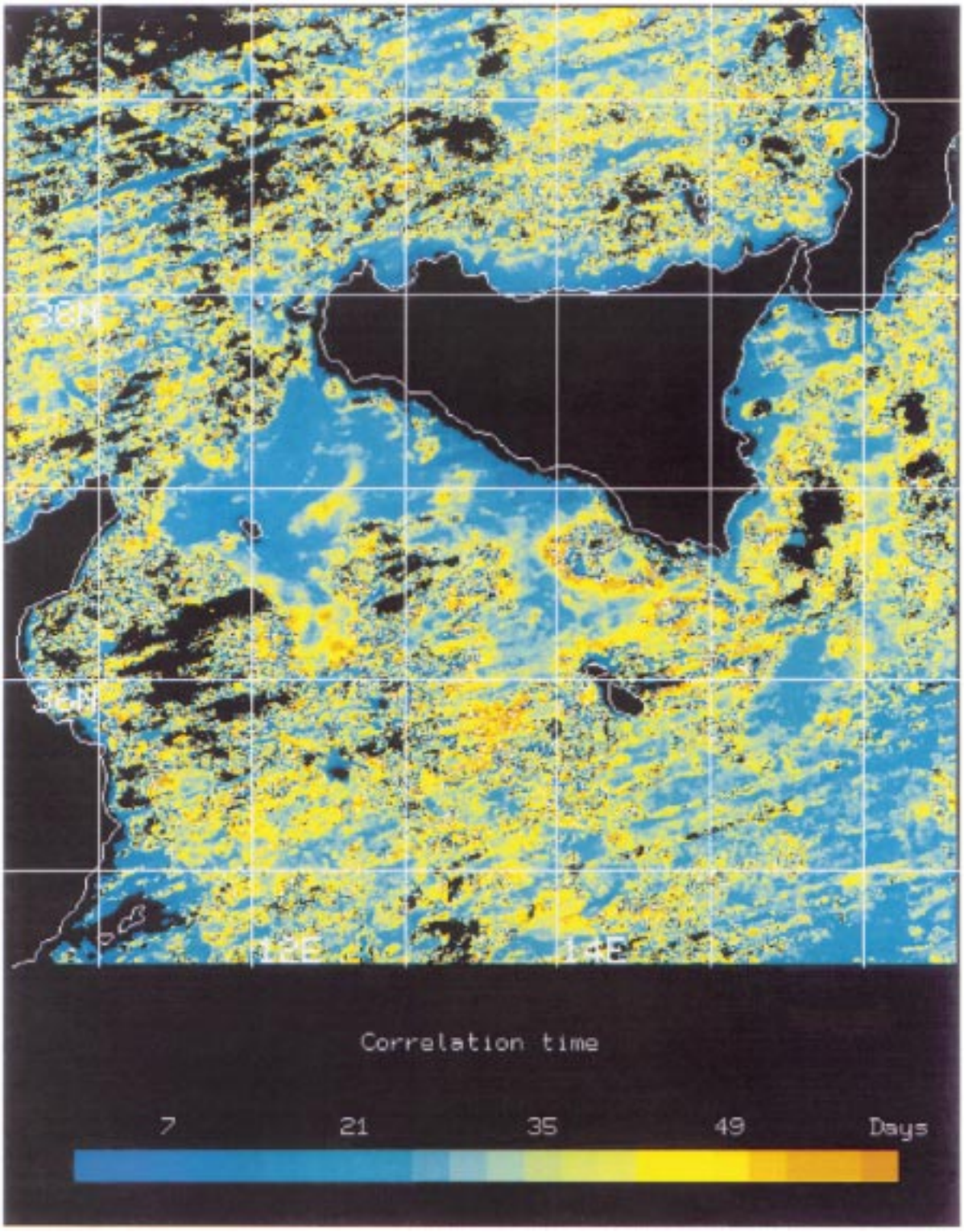

FIG. 2. Spatial distribution of SST correlation times. Times are expressed in days. Mean value is 37 days.

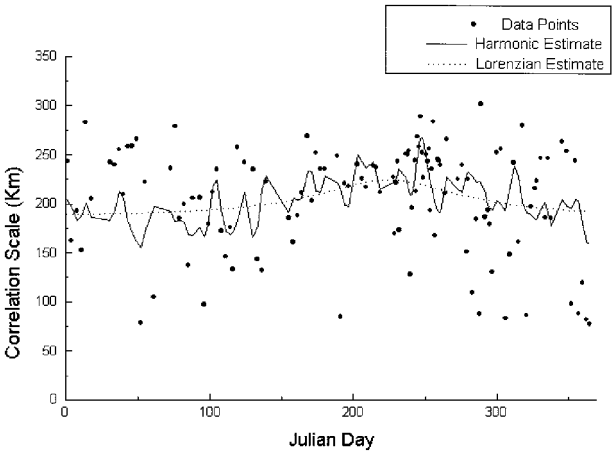

FIG. 3. Time variation of SST spatial scales. Lengths are expressed in kilometers. Dots indicate computed correlation lengths, the solid line indicates the harmonic estimate, and the dashed line the Lorenzian estimate (maximum at day 223).

amplitudes of these harmonics are presented. In order to better resolve the long-term variability of the SST field, the data presented in Fig. 3 (dots) were also fitted with a Lorenzian estimate (dashed line). The maximum of the Lorenzian estimate was at Julian Day 224 (12 August), indicating that the correlation length reaches its maximum during the summer. This seasonal variability is also evident in the monthly means of the SST correlation length (top of Fig. 4).

TABLE 2. Periods and amplitudes of the harmonic estimate of the time variation of the correlation length. Amplitudes are normalized to the total energy (i.e., $\Sigma_1^6 A_i = 1$).

Period (days)	Normalized amplitude
11	0.12
16	0.13
18	0.07
21	0.17
35	0.17
320	0.34

In Fig. 4 (top), the evolution of the monthly mean correlation length of the SST field and of the first four baroclinic Rossby radii (bottom) is shown. The first four baroclinic Rossby radii are characterized by a similar seasonal variation, with the minimum in January and the maximum during summer (from August to October). The first Rossby radius varies from 7.9 km in January to 11.4 km in August and 11.1 km in October. The second Rossby radius varies from 3.6 km in March to 5.6 km in August, while the third and fourth reach their minima in January with 2.3 and 1.5 km, respectively. The maximums of the third and forth modes are shifted by one month, with the third reaching its maximum in September (3.8 km), and the fourth in August (2.9 km).

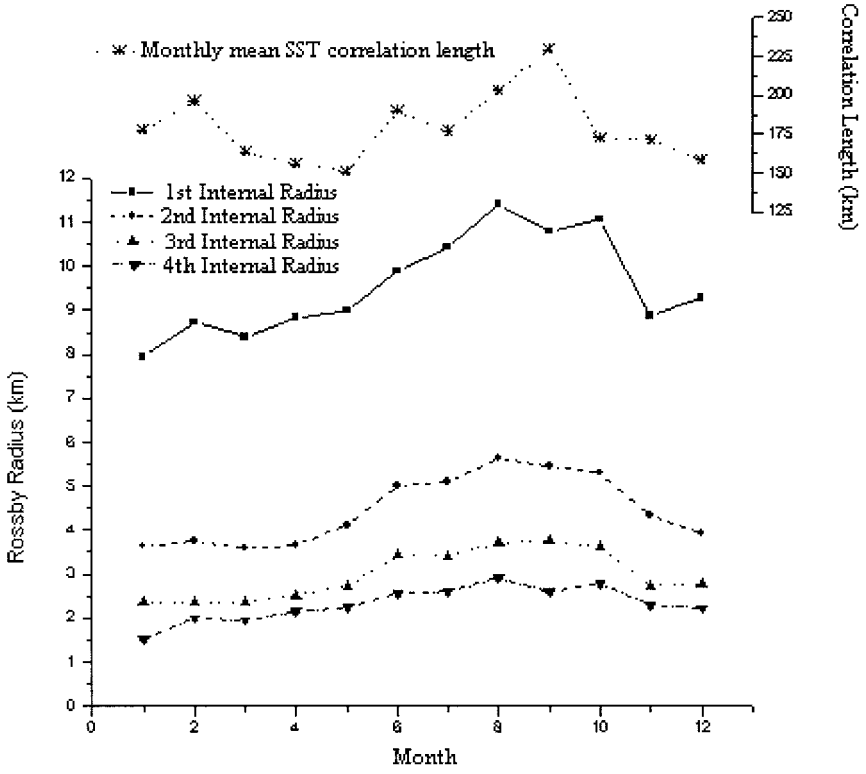

FIG. 4. (Top) Mean monthly correlation lengths expressed in kilometers. (Bottom) Internal deformation radii expressed in kilometers.

It is worth noting that the seasonal variation of the first four Rossby radii is characterized by a slow increase during the winter-to-summer transition and a relatively fast decrease during the summer-to-winter transition. Owing to high values in September of the internal radii, this aspect of the seasonal variability is more pronounced in the first and third modes.

4. Discussion and conclusions

This paper deals with the scales and variability of the SST over the Channel of Sicily. Time- and spatial scales are studied by estimating the SST autocorrelation function from an irregularly spaced dataset with a direct method based on the estimation of averages of different sample products. Scales of the SST distribution are estimated by fitting separately in space and time tabulated values of correlation with a Gaussian function. The result is a bidimensional array of correlation times and an unidimensional array of correlation lengths.

The array of correlation times is noisy, reflecting difficulties in obtaining well-converged results even from large datasets. It is worth noting the occurrence of a low pattern over the Sicilian continental shelf with time values from 7 to 25–30 days. The shape and the timescales of this pattern indicate that it is related to mesoscale features associated with upwelling episodes that characterize this region during summer (Philippe and Harang 1982).

The time variability of SST correlation length can be described by a low-frequency signal (period 320 days), representing the annual cycle, superimposed onto five harmonics with periods from 11 to 35 days. Monthly mean values of the SST correlation length and the first internal radius of deformation exhibit similar time variability, indicating that the long-term variability of the SST correlation length can be related to seasonal variations of the relative influence of different baroclinic components. Differences between the first internal radius and the SST correlation length cycles are not surprising. Indeed, although unstable eddies tend to have scales on the order of the first internal radius or larger, energy tends to cascade over longer scales. Owing to the strong seasonal modulation of the system, statistical equilibrium between different modes is not likely to be achieved throughout the channel. In addition, especially over short timescales, baroclinic instabilities may produce significant differences in these two cycles.

Interpolation of sparse SST observations is commonly accomplished by using objective analysis schemes (Gandin 1965). In this approach, SST in a given space–time point is represented in terms of linear superposition of SST observations in other space–time points, with coefficients depending on the SST autocorrelation function. To interpolate SST observations, it is therefore vital to represent faithfully the SST autocorrelation function. A common approach to this problem consists in adopting a model function depending on some parameters and fixing these parameters in relation to characteristic horizontal scales of motion. When Brunt–Väisälä frequency profiles are available, these scales are represented on the basis of an estimate of the internal deformation radius. However, horizontal scales of motion are the result of a complex interplay between different baroclinic modes and the barotropic one. If the dominant mode is unknown, it is difficult to decide which scales properly model the behavior of the SST ACF. In this paper, an analysis of the relationships of characteristic scales of SST, assessed from satellite images by assuming a Gaussian model function for the SST autocorrelation function, has been presented. It has been shown that differences between spatial scales of correlation of the SST and internal radii of deformation exist, but seasonal variations of the SST spatial correlation length can be explained in terms of Rossby radii seasonal variability.

REFERENCES

Carter, E. F., and A. R. Robinson, 1987: Analysis models for the estimation of oceanic fields. *J. Atmos. Oceanic Technol.,* **4,** 49–74.

Cayula, J. F., and P. Cornillon, 1992: Edge detection algorithm for SST images. *J. Atmos. Oceanic Technol.,* **9,** 67–80.

Cornillon, P. L., and L. Stramma, 1985: The distribution of diurnal sea surface temperature warming events in the western Sargasso Sea. *J. Geophys. Res.,* **90,** 11 811–11 815.

Dahlquist, G., and A. Bjorck, 1974: *Numerical Methods.* Prentice-Hall, 573 pp.

Gandin, L. S., 1965: *Objective Analysis of Meteorological Fields.* Israel Program for Scientific Translations, 242 pp.

Gill, A. E., 1982: *Atmosphere–Ocean Dynamics.* Academic Press, 662 pp.

Grancini, G., and A. Michelato, 1987: Current structure and variability in the Strait of Sicily and adjacent areas. *Ann. Geophys.,* **5,** 75–88.

Leonardi, R., A. Perilli, and R. Santoleri, 1994: SHARK researh study on objective analysis final report. European Space Agency Tech. Rep. 10180/93/YT-I-(SC), ESA/ESRIN, Frascati, Italy, 124 pp.

Manzella, G. M. R., G. P. Gasparini, and M. Astraldi, 1988: Water exchange between the eastern and the western Mediterranean through the Strait of Sicily. *Deep-Sea Res.,* **35,** 1021–1035.

——, T. S. Hopkins, P. J. Minnet, and E. Nacini, 1990: Atlantic water in the Strait of Sicily. *J. Geophys. Res.,* **95,** 1569–1575.

McClain, E. P., 1981: Split window and triple window sea surface temperature determinations from satellite measurements. *Proc. Symp. on Application of Aerospace Remote Sensing in Marine Research,* Woods Hole, MA, Woods Hole Oceanographic Institution, 6–10.

Philippe, M., and L. Harang, 1982: Surface temperature fronts in the Mediterranean from infrared satellite images. *Hydrodynamics of Semi-Enclosed Seas,* J. C. J. Nihoul, Ed., Elsevier, 91–128.

Picco, P., 1988: Climatological atlas of the western Mediterranean. ENEA Tech. Report, CRAM, La Spezia, Italy, 224 pp.

Santoleri, R., E. Böhm, M. E. Schiano, 1994: The sea surface temperature of the western Mediterranean: Historical satellite thermal data. *Seasonal and Interannual Variability of the Western Mediterranean Sea* (*Coastal and Estuarine Studies*), P. La-Violette, Ed., Vol. 46, American Geophysical Union, 155–176.

Tricomi, F. G., 1961: *Istituzioni di Analisi Superiore* (*Metodi Matematici della Fisica*). C. Geroni, Ed., Università di Torino, 560 pp.